Vehicle Headlights Detection Using Markov Random Fields

Wei Zhang, Q.M. Jonathan Wu, and Guanghui Wang

Computer Vision and Sensing Systems Laboratory (CVSSL)
Department of electrical and computer engineering, University of Windsor,
Windsor, Ontario, Canada. N9B 3P4
{weizhang,jwu,ghwang}@uwindsor.ca

Abstract. Vision-based traffic surveillance is an important topic in computer vision. In the night environment, the moving vehicles are commonly detected by their headlights. However, robust headlights detection is obstructed by the strong reflections on the road surface. In this paper, we propose a novel approach for vehicle headlights detection. Firstly, we introduce a *Reflection Intensity Map* based on the analysis of light attenuation model in neighboring region. Secondly, a *Reflection Suppressed Map* is obtained by using Laplacian of Gaussian filter. Thirdly, the headlights are detected by incorporating the gray-scale intensity, *Reflection Intensity Map*, and *Reflection Suppressed Map* into a Markov random fields framework, which is optimized using Iterated Conditional Modes algorithm. Experimental results on typical scenes show that the proposed method can detect the headlights correctly in the presence of strong reflections. Quantitative evaluations demonstrate that the proposed method outperforms the existing methods.

1 Introduction

Vision-based traffic surveillance system extracts useful and accurate traffic information for traffic flow control, such as vehicle count, vehicle flow, and lane changes. The basic techniques for traffic surveillance include vehicle detection and tracking[6-9], surveillance camera calibration, etc. However, most of the state-of-the-art methods are concentrated on the traffic monitoring in the daytime and very few works address the issue of nighttime traffic monitoring.

In the daytime, the vehicles are commonly detected by exploiting the gray scale, color, and motion information. In the nighttime traffic environment, however, the above information becomes invalid, and the vehicles can only be observed by their headlights and rear lights. Furthermore, there are strong reflections on the road surface (as shown in Fig.1), which makes the problem complicated and challenging. In our work, we concentrate on the vehicle headlights detection in gray-scale images.

Several methods have been developed for vehicle headlights detection. In [1], *Cucchiara* and *Piccardi* detected the headlights by applying morphological analysis as well as taking advantage of headlights' shape and size information. The

H. Zha, R.-i. Taniguchi, and S. Maybank (Eds.): ACCV 2009, Part I, LNCS 5994, pp. 169–179, 2010.

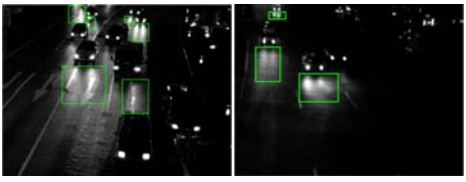

Fig. 1. The strong reflections on the road surface

detected headlights are then verified by matching the headlight symmetry as well as the luminance values along the normal to the main traffic direction. *Chem and Hou* [2] detected rear lights in the nighttime highway, and the reflector spots are removed using the brightness and area filtering. The rear-lights are then paired by using the properties of rear lights and the lanes. *Chen et al.* [3] employed color variation ratio to detect the ground illumination resulted from the vehicle headlights. The headlights information is extracted using a headlight classification algorithm. *Cabani et al.* [4] presented a self-adaptive stereo vision extractor of 3D edges for obstacle, and three kinds of vehicle lights are detected using the $L^*a^*b^*$ color space: rear lights and rear-brake-lights, flashing and warning lights, as well as reverse lights and headlights. *Chen et al.* [5] applied automatic multi-thresholds on the nighttime traffic images to detect the bright objects, which are processed by a rule-based procedure. The vehicles are identified by analyzing their headlights' patterns and the their distances to the camera-assisted car.

In this paper, we present a novel approach for vehicle headlights detection. Firstly, based on the analysis of light attenuation model in neighboring region, we introduce a *Reflection Intensity Map* in which reflections possess much higher intensity than the headlights. Secondly, a *Reflection Suppressed Map* is obtained by using Laplacian of Gaussian filter, and the reflection regions have much lower intensity in the proposed *Reflection Suppressed Map*. Thirdly, the vehicle headlights are detected by incorporating the gray-scale intensity, *Reflection Intensity Map*, and *Reflection Suppressed Map* into a Markov random field (MRF) framework, which is optimized using Iterated Conditional Modes (ICM) algorithm. Experimental results on typical scenes show that the proposed method can detect the headlights correctly in the presence of strong reflections. Quantitative evaluations demonstrate that the proposed method outperforms the state-of-the-art methods.

2 The Features

In common sense, the vehicle headlights possess the highest intensity in the image. However, there may be strong refections on the road surface, which may have as high intensity as the headlights and greatly deteriorate the performance of traditional methods. In this section, we introduce *Reflection Intensity Map* as well as *Reflection Suppressed Map* to discriminate the reflections from the vehicle headlights.

2.1 Reflection Intensity Map

For the light sources in the night environment(such as vehicle headlights), there are commonly atmospheric scattering around the light sources. According to the Bouguers exponential law of attenuation [11], this atmospheric scattering can be modeled as follows.

$$\mathbf{E}(d,\lambda) = I_0(\lambda) \cdot \gamma(\lambda) \cdot \mathtt{exp}(-d); \tag{1}$$

where $I_0(\lambda)$ is the radiant intensity of the light source, $\gamma(\lambda)$ is the total scattering coefficient for wavelength λ, and d is the distance from the light source to the scene point. Considering that the difference between the scattering on different points only depends on d, Equation (1) can be simplified as follows.

$$\mathbf{E}(d,\lambda) = \mathbf{E}_0(\lambda) \cdot \mathtt{exp}(-d); \quad \mathbf{E}_0(\lambda) = I_0(\lambda) \cdot \gamma(\lambda) \tag{2}$$

According to Eq.(2), for a light scattering point $\mathbf{E}(d+\Delta,\lambda)$, we can write it as the follows.

$$\mathbf{E}(d+\Delta,\lambda) = \mathbf{E}(d,\lambda) \cdot \mathtt{exp}(-\Delta); \tag{3}$$

from which we can get the following relationship: for light scattering point $\mathbf{E}(d+\Delta,\lambda)$ of the light source $\mathbf{E}_0$ at a distance of $d+\Delta$, we can consider its light source as $\mathbf{E}(d,\lambda)$ at a distance of Δ. Based on this relationship, we exploit the pixel's neighborhood information to compute the *Reflection Intensity Map*. For pixel (x,y) of image I, we define its interior neighboring region $\Theta^i_{x,y}$ and exterior neighboring region $\Theta^e_{x,y}$ as follows.

$$\begin{aligned} \Theta^i_{x,y} &= \{I(x+u,y+v) \mid 0 \le u \le r, 0 \le v \le r\}; \\ \Theta^e_{x,y} &= \{I(x+u,y+v) \mid 0 \le u \le 2\times r, 0 \le v \le 2\times r\}; \end{aligned} \tag{4}$$

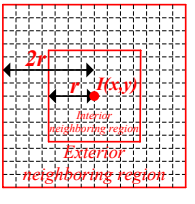

Fig. 2. Interior neighboring region and exterior neighboring region

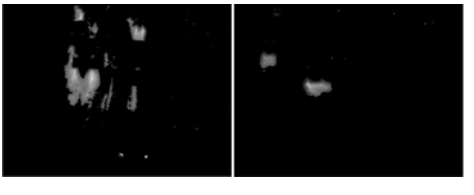

Fig. 3. Two examples of Reflection Intensity Map

in which r is the width of $\Theta^i_{x,y}$, while $\Theta^e_{x,y}$ has a width of $2 \times r$. In Fig.2, we illustrate the defined interior neighboring region and exterior neighboring region. We assume $\Theta^i_{x,y}$ and $\Theta^e_{x,y}$ are in the scattering of the same light source. Let $MI^i_{x,y}$ be the pixel with the minimum intensity in $\Theta^i_{x,y}$, and $MA^i_{x,y}$ be the pixel with the maximum intensity in $\Theta^i_{x,y}$. $MI^i_{x,y}$ can then be deemed as the scatter of $MA^i_{x,y}$ with according to the Eq.(3). The scattering coefficient of $\Theta^i_{x,y}$ can be estimated as follows.

$$\gamma(x,y) = \frac{MI^i_{x,y}}{MA^i_{x,y} \times \mathtt{exp}(-\epsilon^i_{x,y})}; \tag{5}$$

where $\epsilon^i_{x,y}$ is the distance between $MA^i_{x,y}$ and $MI^i_{x,y}$. Assuming the scattering coefficient in $\Theta^e_{x,y}$ is also $\gamma(x,y)$, we then employ the neighborhood $\Theta^e_{x,y}$ to compute the *Reflection Intensity Map* (RI) as follows.

$$RI(x,y) = |MI^e_{x,y} - MA^e_{x,y} \cdot \gamma(x,y) \cdot \mathtt{exp}(-\epsilon^e_{x,y})|; \tag{6}$$

where $MI^e_{x,y}$ and $MA^e_{x,y}$ are the pixel with the minimum and maximum intensity in $\Theta^e_{x,y}$, respectively, and $\epsilon^e_{x,y}$ is the distance between $MA^e_{x,y}$ and $MI^e_{x,y}$.

According to Eq.(3), $MI^e_{x,y}$ can be considered as the scatter of $MA^e_{x,y}$ with scattering coefficient being $\gamma(x,y)$. Apparently, RI should take a low value in headlights' ambient region; in the flat region(including the headlights), the RI also takes a low value because *Reflection Intensity Map* essentially is an edge detection method; in the reflection regions, RI may take on a high intensity. Two examples of the *Reflection Intensity Map* are shown in Fig.3 with the original images given in Fig.1. It can be seen that the strong reflections have much higher intensity than the headlights in the proposed *Reflection Intensity Map*.

2.2 Reflection Suppressed Map

Laplacian of Gaussian (LoG) filter is commonly used for edge detection. In this research, we use LoG filter to obtain the *Reflection Suppressed Map*, and the LoG filter is defined as follows.

$$G(u,v) = \frac{u^2+v^2-2\sigma^2}{\sigma^4} \mathtt{exp}(-\frac{u^2+v^2}{2\sigma^2}); \tag{7}$$

in which σ is the standard deviation. We normalize G to has a unity maximum value and let the results be $\widetilde{G} = \frac{G}{Max(G)}$. The LoG filter is illustrated in Fig.4(a). According to the atmospheric scattering model in [11], the intensity of the light source decreases in a exponential manner [as shown in Fig.4(b)]. When LoG filter is applied on the image, a high value can be obtained in the exponential decreasing region around the headlights, while a negative value in the light source region because of the negative value in the center of LoG filter. Let the negative resultant image of the filter $\widetilde{G}$ applied on image I be S:

$$S = -I \bigotimes \widetilde{G}; \tag{8}$$

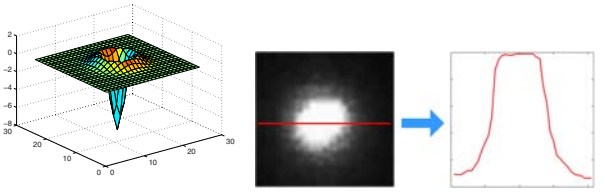

(a) (b)

Fig. 4. (a) the Laplacian of Gaussian filter, (b) the exponential attenuation property of light source

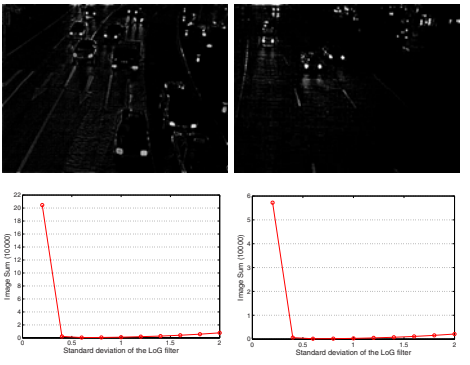

Fig. 5. *Reflection Suppressed Map* and the corresponding F

in which $\bigotimes$ denotes the convolution operation. In this implementation, the parameter σ has a large effect on S, and we calculate the sum of S as F:

$$F = \sum_{(x,y)} S \tag{9}$$

By setting σ to different values, we can obtain F as a function of σ, and σ is set to the value that brings the minimum F. Because $\widetilde{G}$ researches the highest correlation with I when the sum of F researches the minimum.

Because of the property of LoG filter, S commonly has relative higher value on the headlights' boundary, slightly lower value on the headlight, and negative value on the reflections region. Here we implement a flood-fill operation on S to further increase the intensity of headlights region, and let the resultant image be *Reflection Suppressed Map* (RS). In Fig.5, we present two example of RS (first row) as well as the corresponding F (second row)with the original images given in Fig.1. It can be seen that strong reflections have much lower intensity than headlights regions.

We select the headlights pixels and strong reflections pixels in the *'High intensity'* sequence (see Fig.8), and the joint distribution of RI, RS, and I are depicted in Fig.6 using 2441 reflection pixels and 1785 headlights pixels. The strong reflection pixels are selected as those whose intensity is larger than 0.8, and and I, RI and RS are all normalized to range between 0 and 1. From the

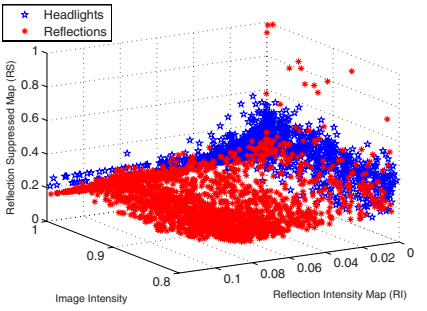

Fig. 6. Distribution of headlights and strong reflections on the image intensity, RS, and RI

figure, we can see that the headlights and reflections have distinct distribution in the proposed feature space.

3 MRF Based Headlights Detection

In this Section, we incorporate RI, RS, and I into a MRF framework to detect the vehicle headlights, and the MRF is optimized by using the ICM algorithm. Because the headlight regions commonly have high intensity, we apply a simple threshold τ on I, and let the resultant pixels be:

$$\kappa = \{(x, y) : I(x, y) > \tau\} \tag{10}$$

The headlights detection is performed on the pixels κ. Therefore, the problem comes down to find the optimal label image Ω based on feature (I, RS, RI). Let $f = (I, RS, RI)$ and Ω has two kinds of labels: headlights α and reflections β. We then attempt to find Ω that maximizes the posterior probability (MAP) $P(\Omega|f)$, according to Bayess theorem, which is proportional to:

$$P(\Omega|f) \propto P(f|\Omega)P(\Omega) \tag{11}$$

The optimal label becomes:

$$\Omega = \texttt{argmax} P(f|\Omega)P(\Omega) \tag{12}$$

In a MRF model, one pixel's label depends on the labels of its neighboring pixels, which is equivalent to a Gibbs process. In according to the the Cliff-Hammersley theorem[12], $P(\Omega)$ with respect to a neighborhood is given as a Gibbs form as follows.

$$P(\Omega) = \tfrac{1}{Z}\texttt{exp}[-U(\Omega_\vartheta)]; \tag{13}$$

in which Z is the the sum of the numerator over labels and U(.) is the energy function. U(.) is commonly formulated as follows.

$$U(\Omega) = \sum_{\kappa}\{\sum_{\vartheta \in \Im_\kappa} [\rho_\kappa \cdot \omega(\Omega_\kappa, \Omega_\vartheta)]\} \tag{14}$$

	4	3	4	
4	2	1	2	4
3	1	κ	1	3
4	2	1	2	4
	4	3	4	

(a)

	$e^{\sqrt{5}}$	e^{-2}	$e^{\sqrt{5}}$	
$e^{\sqrt{5}}$	$e^{\sqrt{2}}$	e^{-1}	$e^{\sqrt{2}}$	$e^{\sqrt{5}}$
e^{-2}	e^{-1}		e^{-1}	e^{-2}
$e^{\sqrt{5}}$	$e^{\sqrt{2}}$	e^{-1}	$e^{\sqrt{2}}$	$e^{\sqrt{5}}$
	$e^{\sqrt{5}}$	e^{-2}	$e^{\sqrt{5}}$	

(b)

Fig. 7. (a) First to forth order neighborhood of site κ, (b) Markov parameters

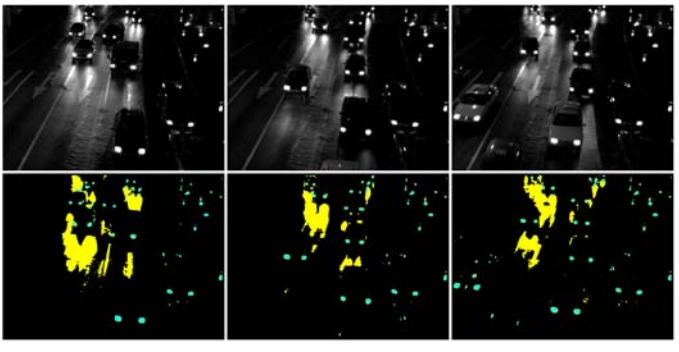

Fig. 8. Experimental Results on the *'High intensity'* sequence

where $\omega(\Omega_\kappa, \Omega_\vartheta) = -1$ if $\Omega_\kappa = \Omega_\vartheta$; and $\omega(\Omega_\kappa, \Omega_\vartheta) = 0$ if $\Omega_\kappa \neq \Omega_\vartheta$; ρ_κ is the Markov parameter; $\Im_\kappa$ is the set of spatial four order cliques (see Fig.7(a)). In this implementation, we set ρ_κ in an exponentially attenuating manner according to Eq.(2), as shown in Fig.7(b). This means that, for site κ, the effect of its neighboring labels decreases exponentially along the neighboring pixels' distance to site κ.

The observed image is commonly acquired through adding a noise process to the true image. Given the perfect image, we can get the density for Ω as:

$$P(f|\Omega) = \prod_{\kappa} P(f_\kappa|\Omega_\kappa) \tag{15}$$

We model the conditional densities $P(f_\kappa|\Omega_\kappa)$ as Gaussian distribution and can get $P(f_\kappa|\Omega_\kappa)$ as follow.

$$\begin{aligned} P(f_\kappa|\Omega_\kappa = \alpha) &= \frac{1}{\sigma_\alpha\sqrt{2\pi}}\exp(-\frac{-(f_\kappa-\mu_\alpha)^2}{2\sigma_\alpha^2}) \\ P(f_\kappa|\Omega_\kappa = \beta) &= \frac{1}{\sigma_\beta\sqrt{2\pi}}\exp(-\frac{-(f_\kappa-\mu_\beta)^2}{2\sigma_\beta^2}) \end{aligned} \tag{16}$$

where μ_α,μ_β,σ_α, and σ_β are the mean value and covariance matrix of the headlights and reflections. We employ the ICM algorithm [10] to obtain solution of Eq.(12). Because ICM uses a 'greedy' algorithm to reach the iterative local minimization, and thus provides us the solution of MAP problem efficiently. Furthermore, ICM can get its convergence in a few iterations.

The Ω is initialized using a random label. In every iteration of ICM, parameters, μ_α,μ_β,σ_α,and σ_β, are updated as follows.

$$\begin{array}{ll} \mu_\alpha = M(f_\kappa|\Omega_\kappa = \alpha) & \mu_\beta = M(f_\kappa|\Omega_\kappa = \beta) \\ \sigma_\alpha = D(f_\kappa|\Omega_\kappa = \alpha) & \sigma_\beta = D(f_\kappa|\Omega_\kappa = \beta) \end{array} \tag{17}$$

in which $M(\cdot)$ and $D(\cdot)$ represent the operations for mean value and covariance matrix calculation, respectively.

4 Experimental Results

We have applied the proposed approach on three typical traffic sequences, *'High intensity'*,*'High speed'*,and *'Rainy'* sequence, to evaluate its effectiveness. In the *'High-speed'* sequence (see Fig.9), the vehicles are moving in a high speed; the *'High intensity'* sequence (see Fig.8) possesses a high traffic intensity; while the *'Rainy'* sequence (see Fig.10) is a rainy scene and has strong reflections on the road surface.

The results of the headlights detection are illustrated in Fig.8-10, in which the vehicle headlights are depicted in cyan and reflections are shown in yellow. We can see that the proposed approach can detect the headlights robustly in all the sequences, and the strong reflections can be differed effectively from the headlights. It should be noted that some interferential objects such as street lamps are also detected.

The performance of the proposed method is also evaluated quantitatively to get a systematic evaluation of the proposed method. Receiver Operator Characteristic (ROC) plots describe the performance of a classifier which assigns input data into dichotomous classes and is selected in the quantitative evaluation of the proposed method. The ROC plot is obtained by testing all possible threshold values, and for each value, plotting the true positive ratio (TPR) on the y-axis against the the false positive ratio (FPR) on the x-axis. The optimal classifier is

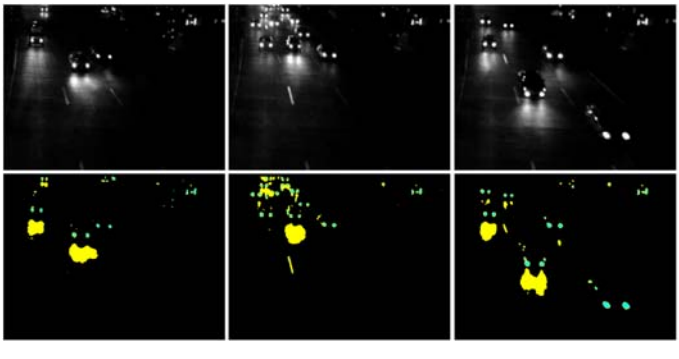

Fig. 9. Experimental Results on the *'High speed'* sequence

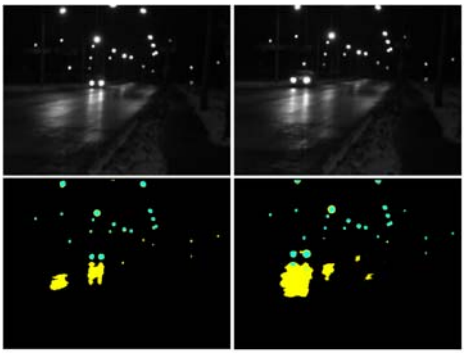

Fig. 10. Experimental Results on the *'Rainy'* sequence

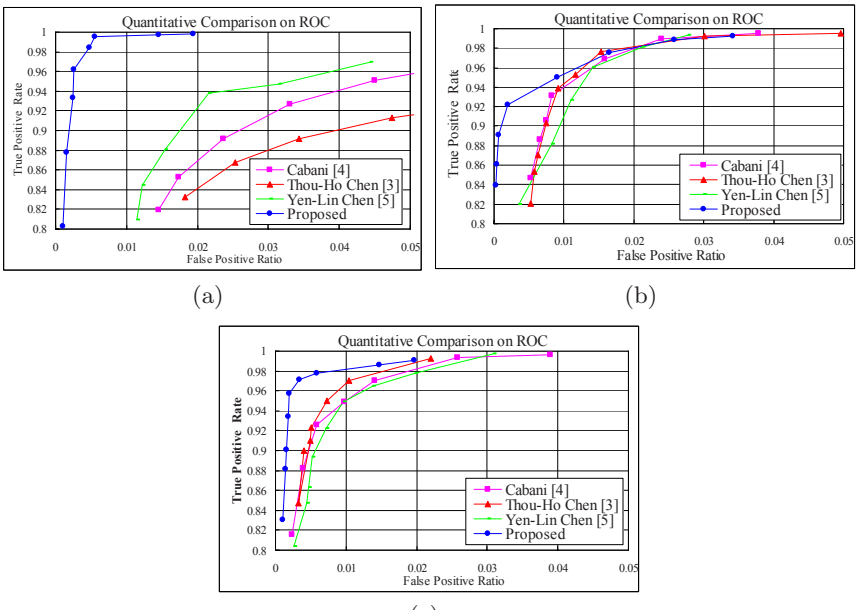

Fig. 11. Quantitative evaluations on (a) *'High intensity'* sequence,(b) *'High speed'* sequence, (c) *'Rainy'* sequence

characterized by an ROC curve passing through the top left corner (0, 1). Here, TPR and FPR are computed as follows:

$$\begin{aligned} TPR &= \frac{\texttt{Truth positives}}{\texttt{The number of headlights pixels in ground truth}} \\ FPR &= \frac{\texttt{False positives}}{\texttt{The number of reflections pixels in ground truth}} \end{aligned} \tag{18}$$

where true positives are the number of headlights pixels that are correctly detected; false positives are the number of reflections pixels that are detected as

headlights; ground truth is the correct detection result and is obtained by manual segmentation in our experiments.

One parameter that affects our algorithm is the threshold τ in Eq.(10) and we tune τ to depict the ROC of the proposed method. We also quantitatively evaluated the methods in [3], [4] and [5] for comparison. For [3], we tune the parameter c in Eq.(5); for [4], we tune the threshold on the L channel of the utilized $L*a*b$ color space; for [5], we tune the multilevel thresholds employed in segmenting bright objects. The resultant ROCs are given in Fig. 11, in which it can be found that the proposed method obviously outperforms other methods in all the sequences.

5 Conclusions

In this paper, we have proposed a robust headlights detection method. *Reflection Intensity Map* is introduced based on the analysis of light attenuation model, and *Reflection Suppressed Map* was obtained by correlating the image with a Laplacian of Gaussian filter. The headlights were detected by incorporating the gray-scale intensity, *Reflection Intensity Map*, and *Reflection Suppressed Map* into a Markov random field framework. Experimental results on typical scenes show that the proposed model can detect the headlights correctly in the presence of strong reflections.

Acknowledgement

This work was particially funded by the Natural Science and Engineering Research Council of Canada.

References

1. Cucchiara, R., Piccardi, M.: Vehicle Detection under Day and Night Illumination. ISCS-IIA 99, 789–794 (1999)
2. Chern, M.-Y., Hou, P.-C.: The lane recognition and vehicle detection at night for a camera-assisted car on highway. In: IEEE International Conference Robotics and Automation (ICRA), September 2003, vol. 2, pp. 2110–2115 (2003)
3. Chen, T.-H., Chen, J.-L., Chen, C.-H., Chang, C.-M.: Vehicle Detection and Counting by Using Headlight Information in the Dark Environment. In: International Conference on Intelligent Information Hiding and Multimedia Signal Processing (IIHMSP), November 2007, vol. 2, pp. 519–522 (2007)
4. Cabani, I., Toulminet, G., Bensrhair, A.: Color-based detection of vehicle lights. In: Intelligent Vehicles Symposium, June 2005, pp. 278–283 (2005)
5. Chen, Y.-L., Chen, Y.-H., Chen, C.-J., Wu, B.-F.: Nighttime Vehicle Detection for Driver Assistance and Autonomous Vehicles. In: International Conference on Pattern Recognition(ICPR), vol. 1, pp. 687–690 (2006)
6. Lou, J.G., Tan, T.N., Hu, W.M., Yang, H., Maybank, S.J.: 3-D model-based vehicle tracking. IEEE Transactions on Image Processing 14, 1561–1569 (2005)

7. Zhang, W., Jonathan Wu, Q.M., Yang, X., Fang, X.: Multilevel Framework to Detect and Handle Vehicle Occlusion. IEEE Transactions on Intelligent Transportation Systems 9, 161–174 (2008)
8. Kato, J., Watanabe, T., Joga, S., Liu, Y., Hase, H.: HMM/MRF-based stochastic framework for robust vehicle tracking. IEEE Transactions on Intelligent Transportation Systems 5, 142–154 (2004)
9. Morris, B.T., Trivedi, M.M.: Learning, Modeling, and Classification of Vehicle Track Patterns from Live Video. IEEE Transactions on Intelligent Transportation Systems 9, 425–437 (2008)
10. Besag, J.E.: On the statistical analysis of dirty pictures. Journal of the Royal Statistical Society. Series B 48, 259–302 (1986)
11. Bouguer, P.: Traité d'optique sur la gradation de la lumière (1729)
12. Geman, S., Geman, D.: Stochastic relaxation: Gibbs distributions and the Bayesian restoration of images. IEEE Transactions on Pattern Analysis and Machine Intelligence 6, 721–741 (1984)